Separation Science and Technology
Publication details, including instructions for authors and subscription information:
http://www.informaworld.com/smpp/title~content=t713708471

# Ternary biosorption equilibria of chromium(VI), copper(II), and cadmium(II) on *Rhizopus arrhizus*

Yeşim Sağ[a]; Burak Akçael[a]; Tülin Kutsal[a]
[a] Department of Chemical Engineering, Hacettepe University, Ankara, Turkey

**To cite this Article** Sağ, Yeşim , Akçael, Burak and Kutsal, Tülin(2002) 'Ternary biosorption equilibria of chromium(VI), copper(II), and cadmium(II) on *Rhizopus arrhizus*', Separation Science and Technology, 37: 2, 279 — 309
**To link to this Article: DOI:** 10.1081/SS-120000789
**URL:** http://dx.doi.org/10.1081/SS-120000789

SEPARATION SCIENCE AND TECHNOLOGY, 37(2), 279–309 (2002)

# TERNARY BIOSORPTION EQUILIBRIA OF CHROMIUM(VI), COPPER(II), AND CADMIUM(II) ON *RHIZOPUS ARRHIZUS*

**Yeşim Sağ,* Burak Akçael, and Tülin Kutsal**

Department of Chemical Engineering, Hacettepe
University, Beytepe, Ankara, Turkey

## ABSTRACT

A process of competitive biosorption of Cr(VI), Cu(II), and Cd(II) ions to *Rhizopus arrhizus* from ternary mixtures was described. Three-dimensional biosorption isotherm surfaces were used to evaluate the three-metal biosorption system performance. Triangular equilibrium diagrams, which could incorporate all the experimental data of the ternary system, were also constructed. The multimetal biosorption equilibria were described by the multicomponent Langmuir and Freundlich models. Of the two models examined, the Langmuir-type model showed the best fit for the three-metal biosorption data, whereas the Freundlich-type multicomponent model did not adequately describe the biosorption results of Cr(VI) ions on *R. arrhizus* from ternary mixtures. The multimetal biosorption results indicated that Cr(VI) and Cu(II) significantly inhibited the biosorption of Cd(II). The Cr(VI)+Cu(II)+Cd(II) combination showed synergistic interaction on the biosorption of Cr(VI) ions.

---

*Corresponding author.

www.dekker.com

*Key Words*: Biosorption; Cadmium(II); Chromium(VI); Copper (II); Multicomponent adsorption models; *Rhizopus arrhizus*; Three-metal system

## INTRODUCTION

Biosorption, the passive non-metabolically mediated process of metal ion binding by living or dead biomass, may serve as a means for purifying industrial waste waters that contain toxic heavy metal ions. Up to now, the research on biosorption of heavy metals has mainly focused on either the adsorption efficiencies and equilibria for different biosorbent materials or the development of batch or continuous biosorption processes (1–5). However, relatively less work has been done to elucidate the details of the biosorption behavior in multimetal systems, which are normally the composition of industrial effluents. Waste waters from plating rinse and bright dip baths contain concentrations ranging over 73–2310 mg $L^{-1}$ Cr(VI), 20–120 mg $L^{-1}$ Cu(II), and 0.1–158 mg $L^{-1}$ Cd(II); 10 000–50 000 mg $L^{-1}$ Cr(VI), 7–44 mg $L^{-1}$ Cu(II), and 2000–5000 mg $L^{-1}$ Cd(II), respectively. Paint manufacturing, ink formulating and dye house waste waters contain Cr(VI), Cu(II), and Cd(II) concentrations ranging from 0.4 to 300 mg $L^{-1}$ Cr(VI), 0 to 100 mg $L^{-1}$ Cu(II), and 0 to 0.81 mg $L^{-1}$ Cd(II) (6).

As mentioned above, very often, there is more than one metal in the solution and, in this case, the assessment of the biosorption performance becomes more complicated, requiring the use of multicomponent isotherm equations (7–10). Two-metal biosorption studies are particularly important for assessing the degree of interference with a biosorption process of common metal ions in wastewaters (11,12). Graphically, two-metal biosorption equilibria can be represented by adding another concentration axis to the conventional biosorption–isotherm plot, and then the isotherm curve will become a three-dimensional biosorption–isotherm surface (13–15). Although this method can be extended to represent three-metal biosorption equilibria, another graphical representation which could incorporate all the experimental data of the ternary system is desirable (8). In this study, the applicabilities of the multicomponent adsorption models to the competitive biosorption equilibria of Cr(VI)–Cu(II)–Cd(II) on *R. arrhizus* were tested. Three-dimensional biosorption isotherm surfaces were created by using an appropriate multicomponent adsorption model. Triangular equilibrium diagrams were constructed. Finally, quantitative details of selective biosorption were discussed in terms of the extent of selectivity or the relative surface coverage of each coadsorbate during selective biosorption.

## EXPERIMENTAL

### Microorganism, Growth Conditions and Preparation of Microorganism for Biosorption

The culture used in this study was the filamentous fungus *R. arrhizus* (US Department of Agriculture culture collection strain no. NRRL 2286). *R. arrhizus* was grown aerobically in batch culture at 30°C in complex medium as described previously (11). After the growth period (96 hr), *R. arrhizus* was washed twice with distilled water, inactivated using 1% formaldehyde, and then dried at 70°C for 24 hr. For biosorption studies, 1.0 g of dried cells were suspended in 100 mL of distilled water and homogenized for 20 min in a homogenizer at 8000 rpm.

### Preparation of Biosorption Media Containing Single and Ternary Metal Ions and Biosorption Studies

Cu(II), Cr(VI), and Cd(II) solutions were prepared by diluting 0.02 *M* of stock solutions of copper(II) and chromium(VI) and 0.01 *M* of stock solution of cadmium(II), obtained by dissolving anhydrous $CuSO_4$, $K_2Cr_2O_7$ or $CdSO_4{\cdot}8H_2O$ in distilled water, respectively. To determine the single-component isotherms, initial metal ion concentrations of Cr(VI), Cu(II), and Cd(II) ions were varied over the 514–4170, 437–3325 and 228–2905 $\mu$mol $L^{-1}$ ranges, respectively while the dry cell weight in each sample was constant at 1.0 g $L^{-1}$. To obtain the required molar ratios, the chosen initial metal ion concentration range for Cr(VI)–Cu(II) and Cd(II) ions corresponds to 25–200 and 50–325 mg $L^{-1}$, respectively, on the basis of weight. pH was adjusted to 2.5 and 4.0 by adding 1.0 *M* of $H_2SO_4$.

To determine multicomponent adsorption isotherms, the initial concentrations of Cd(II) ions were varied between 444 and 3018 $\mu$mol $L^{-1}$ while the Cr(VI) and Cu(II) ion concentrations in each metal mixture were held constant over the 527–2902 and 326–2511 $\mu$mol $L^{-1}$ ranges, respectively. The chosen initial metal ion concentration range for Cr(VI)–Cu(II) and Cd(II) ions corresponds to 25–150 and 50–325 mg $L^{-1}$, respectively, on the basis of weight. Before the solutions were mixed with the fungal suspension, pH was adjusted to 4.0 by adding 1.0 *M* of $H_2SO_4$.

The fungal suspension (20 mL) was mixed with 180 mL of the desired metal solution in an Erlenmeyer flask. The flasks were agitated on a shaker at 25°C for 48 hr, which was sufficiently long for adsorption equilibrium. Agitation rate was 150 rpm. Standard batch biosorption equilibrium methodology applied has been described elsewhere (11,16).

### Measurement of Heavy Metal Ions

The concentration of unadsorbed Cr(VI) and Cu(II) ions in the biosorption medium was determined spectrophotometrically. The colored complexes of Cr(VI) ions with diphenyl carbazide and Cu(II) ions with sodium diethyl dithiocarbamate were read at 540 and 460 nm, respectively (17). The concentration of unadsorbed Cd(II) ions in the sample supernatant was determined using an atomic absorption spectrophotometer (ATI-UNICAM 929, England) with an air–acetylene flame. A PHOTRON Cd(II) hollow cathode lamp (Australia) was used. Cd(II) was measured at 228.8 nm.

## RESULTS AND DISCUSSION

### Models for Biosorption Equilibrium in Single-Metal Systems

The Langmuir isotherm model has the form (18,19):

$$q_{\mathrm{eq}} = \frac{aC_{\mathrm{eq}}}{1 + KC_{\mathrm{eq}}} \tag{1}$$

where $C_{\mathrm{eq}}$ is the metal concentration in solution, $q_{\mathrm{eq}}$ the adsorbed metal ion quantity per unit weight of dried biomass at equilibrium and $a = q_{\max}K$.

The Freundlich equation is commonly presented as (18,19):

$$q_{\mathrm{eq}} = a^0 C_{\mathrm{eq}}^{b^0} \tag{2}$$

where $a^0$ and $b^0$ are the Freundlich constants.

The three-parameter empirical isotherm proposed by Redlich and Peterson is (20):

$$q_{\mathrm{eq}} = \frac{K_R C_{\mathrm{eq}}}{1 + a_R C_{\mathrm{eq}}^{\beta}} \tag{3}$$

where the exponent $\beta$ lies between 0 and 1. When $\beta = 1$, the Redlich–Peterson equation reduces to the Langmuir equation.

### Models for Competitive Biosorption Equilibria in Multimetal Systems

The first multicomponent adsorption model tested in this study is a multicomponent version of the traditional Langmuir isotherm (20,21). The major assumption of this model is that the surface sites are uniform, so that the adsorbates (Cr(VI), Cu(II), and Cd(II)) compete for the same surface sites. The final expression of the multicomponent Langmuir model can be described as follows:

$$q_{i,\mathrm{eq}} = \frac{q_{\max} K_i C_{i,\mathrm{eq}}}{1 + K_i C_{i,\mathrm{eq}} + K_j C_{j,\mathrm{eq}} + K_k C_{k,\mathrm{eq}}} \tag{4}$$

In this model, the maximal capacity $q_{\max}$ is universal so that all three metals obey the fundamental hypothesis of the Langmuir model.

The Freundlich type adsorption isotherm for component $i$ in a $k$-component system is written in the form (22):

$$q_{i,\mathrm{eq}} = a_i^0 C_{i,\mathrm{eq}} \left( \sum_{j=1}^{k} a_{ij} C_{j,\mathrm{eq}} \right)^{b_i^0 - 1} \tag{5}$$

The pre-exponential coefficient $a_i^0$ and the exponent $b_i^0$ are determined from the monocomponent systems. The competition coefficients $a_{ij}$ describe the inhibition to the adsorption of component $i$ by component $j$, and can be determined from thermodynamic data or, more likely, from experimental data of multicomponent systems. The assumptions incorporated in the derivation are: (a) each component individually obeys Eq. (2); (b) for each component in a multicomponent adsorption, there exists an exponential distribution of adsorption energies of sites,

$$N_i(Q) = \alpha_i \exp(-n_i Q/RT) \tag{6}$$

where $\alpha_\mathrm{i}$ and $n_i$ are constants; and (c) the coverage by each sorbate at each energy level $Q$ is given by the multicomponent Langmuir isotherm:

$$\theta_i(Q) = \frac{K_i C_{i,\mathrm{eq}}}{1 + \sum K_j C_{j,\mathrm{eq}}} \tag{7}$$

$$K_j = K_{0j} \exp(Q/RT) \tag{8}$$

Integration of $N_i(Q)\theta_i(Q)$ over energies in the range $-\infty$ to $\infty$ yields Eq. (5) and the competition coefficients are defined as $a_{ij} = K_{0j}/K_{0i}$ and thus $a_{ji} = 1/a_{ij}$. For ternary systems, according to the proposed model (22–24)

$$a_{12} a_{23} a_{31} = \frac{K_{02}}{K_{01}} \cdot \frac{K_{03}}{K_{02}} \cdot \frac{K_{01}}{K_{03}} = 1 \tag{9}$$

The adsorption of each component in a three-component system is

$$q_{1,\mathrm{eq}} = a_1^0 C_{1,\mathrm{eq}} (C_{1,\mathrm{eq}} + a_{12} C_{2,\mathrm{eq}} + a_{13} C_{3,\mathrm{eq}})^{b_1^0 - 1} \tag{10a}$$

$$q_{2,\mathrm{eq}} = a_2^0 C_{2,\mathrm{eq}} (a_{21} C_{1,\mathrm{eq}} + C_{2,\mathrm{eq}} + a_{23} C_{3,\mathrm{eq}})^{b_2^0 - 1} \tag{10b}$$

$$q_{3,\mathrm{eq}} = a_3^0 C_{3,\mathrm{eq}} (a_{31} C_{1,\mathrm{eq}} + a_{32} C_{2,\mathrm{eq}} + C_{3,\mathrm{eq}})^{b_3^0 - 1} \tag{10c}$$

### Quantitative Analysis of Selective Biosorption

To quantify the synergistic and antagonistic behavior, the relative metal *i* biosorption is defined (25).

$$R_i = \frac{\text{metal } i \text{ biosorption capacity with the coexistence of metal } j \text{ and } k}{\text{metal } i \text{ biosorption capacity without the coexistence of metal } j \text{ and } k} \times 100\% \tag{11}$$

If the interactive effects of a mixture of metals are synergistic, $R_i\% > 100$, antagonistic, $R_i\% < 100$, and noninteractive, $R_i\% = 100$. The experimental data are also presented in terms of the individual biosorption efficiency ($Y_\mathrm{i}\%$) (11), the total biosorption efficiency ($Y_\mathrm{t}\%$) (26), and the relative coverage ($\theta_i\%$) (25), whose definitions are as follows:

$$Y_\mathrm{i} = \frac{\text{concentration of metal } i \text{ biosorbed}}{\text{initial concentration of metal } i} \times 100\% \tag{12}$$

$$Y_\mathrm{t} = \frac{\text{total concentration of metal ions biosorbed}}{\text{total initial metal ion concentration}} \times 100\% \tag{13}$$

$$\theta_i = \frac{\text{moles of metal } i \text{ biosorbed}}{\text{moles of all three metals biosorbed}} \times 100\% \tag{14}$$

The values of $Y_\mathrm{i}\%$ and $\theta_i\%$ are indications of the relative biosorption preference and distribution of each metal of interest on the biosorbent.

### Cr(VI), Cu(II), and Cd(II) Biosorption on *R. arrhizus*: Single-Metal Situation

The effect of pH on the single-metal biosorption of Cr(VI), Cu(II), and Cd(II) ions by *R. arrhizus* was investigated in strong acidic (pH 2.5) and weak acidic (pH 4.0) synthetic aqueous solutions. The monocomponent equilibrium data were analyzed using the Langmuir, Redlich–Peterson, and Freundlich isotherms. It is clear that the Langmuir constants, $q_{\max}$ and $K$, the Redlich–Peterson constants, $K_R$ and $a_R$, and the Freundlich constant, $a^0$, for Cu(II) and Cd(II) ions increased with increase in pH. Optimum pH for the biosorption of Cu(II) and Cd(II) ions by *R. arrhizus* was determined as 4.0, whereas higher biosorptive uptake of Cr(VI) ions by *R. arrhizus* was obtained at pH 2.5 (Tables 1–3).

The Langmuir equation was linearized by plotting $1/q_{eq}$ vs. $1/C_{eq}$ to determine the Langmuir constants from the slope $1/a$ and the intercept $K/a$. The Langmuir equation allows easy expression of the saturation metal uptake ($q_{\max}$) and the Langmuir coefficient, $K$, a ratio of the adsorption rate constant to the desorption rate constant. The biomass had the highest saturation capacity for Cu(II) at pH 4.0 in the single-metal system, followed by Cr(VI) at pH in the range 2.5–4.0, and Cd(II) at pH 4.0.

The three parameters given by the Redlich–Peterson adsorption model were estimated from the monocomponent adsorption data of Cr(VI), Cu(II), and Cd(II) ions by using an MS EXCEL 97 computer program. It can be seen that in the monocomponent biosorption of Cd(II) ions at pH in the range 2.5–4.0, the value of $\beta$ tends to unity, that is the isotherm is approaching the Langmuir form.

Finally, the intercept of the linearized Freundlich equation, $a^0$, is an indication of the sorption capacity of the sorbent; the slope, $b^0$, indicates the effect of concentration on the sorption capacity and represents the sorption intensity. As the values of adsorption capacity, $a^0$, and intensity, $b^0$, for Cr(VI) and Cu(II) ions are found to be very close to each other, these values also indicate a decidedly better biomass affinity for, and higher biosorption of, Cr(VI) and Cu(II) ions vs. Cd(II) ions.

To quantify the agreement between the model predictions and experimental observations, four different statistical methods were used: the relative percentage error (RPE) (16,27), the variance (MSR) (25), the objective function ($E_i$) (8), and the regression coefficient ($R$). Comparing the values of RPE, MSR, $E_i$, and $R$ shows that the single-component Freundlich model provided the best correlation for the biosorption of Cr(VI) ions on *R. arrhizus*, while the best fit for the Cu(II) and Cd(II) ions was obtained by using the single-component Langmuir model. Due to existence of a large number of active sites on the biomass having high specificity for Cr(VI) in a wide pH range, wastewaters containing Cr(VI), Cu(II), and Cd(II) ions together can be treated with *R. arrhizus* at pH 4.0 rather than pH 2.5. In addition, the pH of industrial wastewaters containing these metal ions changes in the range 3.0–5.0. It should also be noted that at pH values higher than 5.5, Cu(II) ions precipitated and biosorption studies at these pH values could not be performed.

**Table 1.** The Comparison of the Individual Constants Obtained from the Single-Component Langmuir, Redlich–Peterson, and Freundlich Adsorption Isotherms for Cr(VI) Ions at Different pH Values

| Langmuir model<br>pH | $q_{\max}$ (μmol g$^{-1}$) | $K$ (L μmol$^{-1}$) | $a$ (L g$^{-1}$) | RPE (%)[a] | MSR[b] | $E_i$[c] | $R$ |
|---|---|---|---|---|---|---|---|
| 2.5 | 504 | 0.0029 | 1.4830 | 8.9 | 2106 | 0.07 | 0.855 |
| 4.0 | 368 | 0.0026 | 0.9710 | 7.8 | 565 | 0.05 | 0.864 |
| Redlich–Peterson model | | | | | | | |
| pH | $K_R$ (L g$^{-1}$) | $a_R$ (μmol$^{\beta+1}$ g$^{-1}$ L$^{-\beta}$) | $\beta$ | RPE (%) | MSR | $E_i$ | $R$ |
| 2.5 | 2.2628 | 0.0103 | 0.8980 | 7.1 | 1525 | 0.05 | 0.741 |
| 4.0 | 5.5802 | 0.1263 | 0.7391 | 3.7 | 231 | 0.03 | 0.939 |
| Freundlich model | | | | | | | |
| pH | $a^0$ (μmol$^{1-b^0}$L$^{b^0}$g$^{-1}$) | $b^0$ | RPE (%) | MSR | $E_i$ | $R$ | |
| 2.5 | 38.70 | 0.3190 | 5.1 | 414 | 0.02 | 0.961 | |
| 4.0 | 27.60 | 0.3193 | 4.7 | 222 | 0.02 | 0.948 | |

[a] Relative percent error:

$$\text{RPE}\,(\%) = \frac{\sum[|(q_{i,\text{eq}})_{\text{predicted}} - (q_{i,\text{eq}})_{\text{experimental}})|/(q_{i,\text{eq}})_{\text{experimental}}] \times 100}{N}$$

where $N$ is the number of experimental data.

[b] Mean square of residuals:

$$\text{MSR} = \frac{\sum[(q_{i,\text{eq}})_{\text{predicted}} - (q_{i,\text{eq}})_{\text{experimental}}]^2}{N}.$$

[c] Objective function:

$$E_i = \sum_{j=1}^{N}\left[\frac{(q_{i,\text{eq}})_{\text{experimental}} - (q_{i,\text{eq}})_{\text{predicted}}}{(q_{i,\text{eq}})_{\text{experimental}}}\right]^2.$$

*Table 2.* The Comparison of the Individual Constants Obtained from the Single-Component Langmuir, Redlich–Peterson, and Freundlich Adsorption Isotherms for Cu(II) Ions at Different pH Values

| Langmuir model | | | | | | | |
|---|---|---|---|---|---|---|---|
| pH | $q_{\max}$ (μmol g$^{-1}$) | $K$ (L μmol$^{-1}$) | $a$ (L g$^{-1}$) | RPE (%) | MSR | $E_i$ | $R$ |
| 2.5 | 149 | 0.0013 | 0.1983 | 4.2 | 36 | 0.02 | 0.982 |
| 4.0 | 567 | 0.0015 | 0.8373 | 2.5 | 114 | 0.01 | 0.974 |
| Redlich–Peterson model | | | | | | | |
| pH | $K_R$ (L g$^{-1}$) | $a_R$ (μmol$^{\beta+1}$ g$^{-1}$ L$^{-\beta}$) | $\beta$ | RPE (%) | MSR | $E_i$ | $R$ |
| 2.5 | 0.3482 | 0.0114 | 0.8173 | 5.8 | 51 | 0.03 | 0.895 |
| 4.0 | 1.0628 | 0.0044 | 0.8804 | 2.1 | 139 | 0.01 | 0.973 |
| Freundlich model | | | | | | | |
| pH | $a^0$ (μmol$^{1-b^0}$L$^{b^0}$$g^{-1}$) | $b^0$ | RPE (%) | MSR | $E_i$ | $R$ | |
| 2.5 | 5.31 | 0.3940 | 8.5 | 83 | 0.05 | 0.891 | |
| 4.0 | 31.65 | 0.3391 | 4.0 | 260 | 0.01 | 0.936 | |

***Table 3.*** The Comparison of the Individual Constants Obtained from the Single-Component Langmuir, Redlich–Peterson, and Freundlich Adsorption Isotherms for Cd(II) Ions at Different pH Values

| Langmuir model<br>pH | $q_{\max}$ (μmol g$^{-1}$) | $K$ (L μmol$^{-1}$) | $a$ (L g$^{-1}$) | RPE (%) | MSR | $E_i$ | $R$ |
|---|---|---|---|---|---|---|---|
| 2.5 | 177 | 0.0035 | 0.6161 | 4.2 | 46 | 0.03 | 0.969 |
| 4.0 | 236 | 0.0036 | 0.8418 | 3.9 | 67 | 0.01 | 0.990 |
| Redlich–Peterson model | | | | | | | |
| pH | $K_R$ (L g$^{-1}$) | $a_{\mathrm{R}}$ (μmol$^{\beta+1}$ g$^{-1}$ L$^{-\beta}$) | $\beta$ | RPE (%) | MSR | $E_i$ | $R$ |
| 2.5 | 0.6351 | 0.0042 | 0.9770 | 3.3 | 42 | 0.03 | 0.958 |
| 4.0 | 0.9747 | 0.0076 | 0.9203 | 2.8 | 58 | 0.01 | 0.973 |
| Freundlich model | | | | | | | |
| pH | $a^0$ (μmol$^{1-b^0}$L$^{b^0}$g$^{-1}$) | $b^0$ | RPE (%) | MSR | $E_i$ | $R$ | |
| 2.5 | 13.83 | 0.3251 | 7.2 | 106 | 0.05 | 0.921 | |
| 4.0 | 16.81 | 0.3395 | 7.3 | 185 | 0.05 | 0.933 | |

## Models for Competitive Biosorption Equilibria of Cr(VI), Cu(II), and Cd(II) Ions in Ternary Systems

### Multicomponent Langmuir Model

To examine the validity of the Langmuir model for multicomponent adsorption systems, the experimental data of the ternary system were simulated numerically according to Eq. (4). Four parameters, $q_{\max}$, $K_{\mathrm{Cr}}$, $K_{\mathrm{Cu}}$ and $K_{\mathrm{Cd}}$, associated with the Langmuir model were estimated by utilizing MS EXCEL 97 numerical analysis program. The optimal parameters were evaluated by minimizing the mean square of residuals. A higher value of the $K_i$ parameter for Cu(II) and Cr(VI) than for Cd(II) implies that the biosorbent had a higher affinity for Cu(II) and Cr(VI) than for Cd(II) (Table 4). Higher values of $K_i$ also correspond to a higher ratio of adsorption and desorption rate constants. It can be concluded that there is stronger biosorption by the biosorbent of Cu(II) and Cr(VI) than of Cd(II). These results further confirm that biosorption of Cu(II) was most favored by the biomass at pH 4.0, but which had the least preference for Cd(II), in agreement with the single-component data. Deviations of the experimental points from those predicted by the multicomponent Langmuir model are generally small. Among the three components, the predictions for the Cd(II) uptake are the least accurate. Since the amounts of Cd(II) adsorbed per unit weight of microorganism at equilibrium were very low, the relative percentage errors between the experimental and predicted values for Cd(II) increased, whereas the mean of sum of squared residuals decreased. The best fit was obtained for Cr(VI) ions and the relative percentage error and the variance between the experimental data and the Langmuir model predictions decreased with respect to single-component Cr(VI) system.

The maximal total capacity, $q_{\max}$, resulting from single systems was $567\,\mu\mathrm{mol\,g^{-1}}$ (for Cu(II) alone) and $1171\,\mu\mathrm{mol\,g^{-1}}$ (the sum of the maximal total capacities of Cr(VI), Cu(II), and Cd(II) ions). The maximal total capacity, $q_{\max}$, resulting from ternary systems was $928\,\mu\mathrm{mol\,g^{-1}}$ (for Cr(VI)+Cu(II)+Cd(II)). For this reason, the adsorption sites of Cr(VI), Cu(II), and Cd(II) in ternary systems were likely to be partially overlapped. On the other hand, the sum of the maximal total capacities of Cr(VI), Cu(II), and Cd(II) ions resulting from single systems was slightly greater than the maximal total capacity resulting from ternary systems. It may also imply that there exist a variety of binding sites on the biomass that are partially specific for individual metal species. In trimetallic combination, sorption of metals is a competitive process between ions in solution and those sorbed onto the biomass surface. Antagonistic interaction of the metals could be due to the fact that different metal ions have different affinities to cell binding sites, therefore the effective binding sites available for a single metal are reduced. The information provided from maximal capacities seems to violate

***Table 4.*** Kinetic Parameters of Multicomponent Adsorption Isotherms Estimated from Multicomponent Langmuir Model

| $i$ (Metal ion) | $q_{\max}$ ($\mu$mol g$^{-1}$) | $K_i\times10^4$ (L $\mu$mol$^{-1}$) | RPE (%) | MSR | $E_i$ |
|---|---|---|---|---|---|
| Cd–Cr–Cu | 928 | $K_{Cd}$ = 3.59 | 8.7 | 146 | 0.26 |
| | | $K_{Cr}$ = 9.35 | 5.7 | 357 | 0.12 |
| | | $K_{Cu}$ = 9.99 | 7.1 | 309 | 0.19 |
| | | | Average = 7.1 | Average = 270 | Average = 0.19 |

basic assumptions of the Langmuir model, which proposes that the entire adsorbent surface is homogeneous and that there is no lateral interaction between adsorbate molecules, and thus the affinity of each binding site for the adsorbate molecules should be uniform. On the other hand, the Freundlich model is an empirical model assuming a logarithmic decrease in the heat of sorption with the fraction of surface covered by the sorbed solute. Biological surfaces are thought to have heterogeneous energies for sorbing metals. For this reason, the competitive biosorption behavior of the three metals examined was further investigated by using the multicomponent Freundlich model.

## The Multicomponent Freundlich Model

The competition coefficients of the multicomponent Freundlich model ($a_{12}$, $a_{13}$, $a_{21}$, $a_{23}$, $a_{31}$ and $a_{32}$) given by Eqs. (10a)–(c) were estimated from the competitive biosorption data of Cr(VI), Cu(II), and Cd(II) ions by using MS EXCEL 97 numerical analysis program (Table 5). The good agreement of the adsorption equilibrium data of Cu(II) and Cd(II) ions with the multicomponent Freundlich model was demonstrated and by the observation that the product of the competition coefficients $a_{12}\cdot a_{23}\cdot a_{31}$ is close to unity for the ternary system Cr(VI)–Cu(II)–Cd(II). Comparing the competition coefficients in this table shows that Cr(VI) significantly inhibited the biosorption of Cd(II) ($a_{12} = 1.6100$), while the uptake of the strongly adsorbed Cr(VI) was almost unaffected by the presence of Cd(II) ($a_{21} = 0.0100$). Whereas Cu(II) obviously interfered with the Cr(VI) uptake ($a_{23} = 0.9600$), upon quantitative analysis it can be easily seen that it did so much more than vice versa ($a_{32} = 0.0100$). On the other hand, a significant reduction in the Cu(II) uptake was observed by the presence of Cd(II) ($a_{31} = 0.6500$).

Although the multicomponent Freundlich model for ternary metal mixtures represented most the adsorption equilibrium data of Cu(II) and Cd(II) ions on *R.*

*arrhizus* satisfactorily, the model was not successful enough to define the competitive biosorption behavior of Cr(VI) ions from the ternary mixtures. Since the expected increases in the inhibitory effects caused by the presence of the other metal ions at increasing concentrations were not observed, the predicted equilibrium uptake values for Cr(VI) ions were lower than the experimental equilibrium uptake values. The RPE, MSR and $E_i$ between the experimental and predicted values using the multicomponent Freundlich model increased considerably especially in the case of Cr(VI), compared with those obtained using the multicomponent Langmuir model. As a result, comparison of the values of statistical parameters using to test the accuracy of the multicomponent adsorption models shows clearly that the multicomponent Langmuir model provided the best correlation for the biosorption of the three metal ions on *R. arrhizus.*

### Graphical Representation of the Ternary Biosorption Equilibrium Data: Construction of Triangular Equilibrium Diagrams and 3-D Biosorption Isotherm Plots

The possibility of using a triangular diagram to graphically depict the equilibrium data of the Cr(VI)+Cu(II)+Cd(II) system was tested. To use the triangular diagram, the equilibrium data were converted into their respective dimensionless forms by using mole fractions. The final residual concentrations, $C_{i,\mathrm{eq}}$, and the metal uptakes, $q_{i,\mathrm{eq}}$, were converted to metal mole fractions in solution, $x(i)$, and metal mole fractions in the biosorbent, $y(i)$, respectively. The experimental and predicted metal uptakes using the multicomponent Langmuir model are shown in Fig. 1(a)–(c). In the triangular diagram, the equidistant axes refer to the mole fractions of the respective metal species on the biosorbent. Contour lines or parametric lines which, in Fig. 1(a)–(c), correspond to the mole fractions of Cr(VI), Cu(II), and Cd(II) in solution, respectively are superimposed on these axes. Due to the preference of *R. arrhizus* for the metals examined which was Cu(II) $\geq$ Cr(VI) $>$ Cd(II), the experimental points tend to cluster toward the Cr(VI) and Cu(II) corners with a noticeable void in the Cd(II) corner of the triangular diagram. The predicted and experimental metal uptakes are quite consistent over a large range of the residual concentrations of the three metals.

A ternary system can also be represented by using 3-D graphs whereby the effect of the third ion is ignored, because there is a preferential biosorbent selectivity for Cr(VI) and Cu(II) over Cd(II). A 3-D diagram based on randomly generated experimental data is plotted and the data are fitted a smooth surface according to the appropriate input equation, which represents the surface. In this stage, the input equation is the ternary Langmuir-type equation, which created the biosorption isotherm surfaces seen in Fig. 2(a)–(c), and smoothed and fitted to

***Table 5.*** Kinetic Parameters of Multicomponent Adsorption Isotherms Estimated from Multicomponent Freundlich Model

| $i$ | Metal | $a^0$ | $b^0$ | $a_{i1}$ | $a_{i2}$ | $a_{i3}$ | RPE (%) | MSR | $E_i$ |
|---|---|---|---|---|---|---|---|---|---|
| 1 | Cd(II) | 16.81 | 0.3395 | 1.0 | 1.6100 | 0.0100 | 11.6 | 1367 | 0.62 |
| 2 | Cr(VI) | 27.60 | 0.3193 | 0.0100 | 1.0 | 0.9600 | 34.2 | 13282 | 3.23 |
| 3 | Cu(II) | 31.65 | 0.3391 | 0.6500 | 0.0100 | 1.0 | 10.6 | 709 | 0.51 |
|  |  |  |  |  | $a_{12} \cdot a_{23} \cdot a_{31} = 1.005$ |  | Average = 18.8 | Average = 5120 | Average = 1.45 |

experimental biosorption data. Empirically selected initial concentrations of Cd(II) ($C_{\mathrm{Cd(II),i}}$ was held constant over the 453–2914 μmol L$^{-1}$ range) were chosen as parameters and the two biosorption isotherm surfaces of the Cr(VI)+Cu(II) systems were depicted in Fig. 2(a)–(b). Depending on the $q_{i,\mathrm{eq}}$ value calculated and used, there could be three different biosorption–isotherm surface plots: (1) for the uptake of Cr(VI), yielding the effect of Cu(II) on Cr(VI); (2) for the uptake of Cu(II), yielding the effect of Cr(VI) on Cu(II); and (3) for the total uptake (Cr(VI)+Cu(II)). The adsorption model used for smoothing of the biosorption isotherm surfaces makes it possible to eventually derive two-dimensional (2-D) biosorption isotherm curves from the complex 3-D image by cutting through it by a series of parallel 'isoconcentration' planes for selected concentrations of one or the other metal, respectively (12,28). The resulting set of biosorption isotherm curves depicts either the effect of the second metal on the biosorption of the first one or vice versa. For example, Fig. 3, the effect of Cu(II) on the uptake of Cr(VI), was derived by 'cutting' the isotherm surface with Cu(II) isoconcentration planes and plotting the resulting curves.

As seen in Figs. 2(a) and 3, a significant reduction in the Cr(VI) uptake was observed only at relatively high Cu(II) and Cd(II) concentrations. Similarly and conversely, the effect of Cr(VI) on the uptake of Cu(II) is seen in Fig. 4 showing the 'isoconcentration cuts' of the Cu(II) biosorption isotherm surface from Fig. 2(b). Figure 2(c) depicts total metal uptake behavior as a function of the two-metal equilibrium concentration (Cr(VI) and Cu(II)) with the other metal equilibrium concentration (Cd(II)) as a parameter. In this figure, the two main planes ($x$–$z$ and $y$–$z$) show the single-metal biosorption isotherms for Cr(VI) and Cu(II), respectively. The lowest isotherm curves in Fig. 2(c) represent simple single-metal biosorption isotherms for Cr(VI) and Cu(II), respectively. Even if one type of the metal ion present interfered with the uptake of another one in the system, the overall total metal uptake was not lowered. Figure 2(c) also shows that, with high levels of overall metal concentration present in the solution, *R. arrhizus* easily reaches the saturation level demonstrated by a wide plateau of the surface. More detailed examination of the 3-D surface plots again confirms the higher affinity of this biosorption system for Cu(II) and Cr(VI) at pH 4.0 as quantitatively expressed previously. The unsaturated *R. arrhizus* demonstrates itself in the low-concentration region of the plots by sharply lower metal uptake by the solid phase.

In Fig. 5(a)–(c), unadsorbed Cr(VI) and Cd(II) ion concentrations in solution at equilibrium are plotted against the Cr(VI), Cd(II), and total metal uptakes, respectively. The initial concentrations of Cu(II) ions were held constant over the 390–2399 μmol L$^{-1}$ range. A similar biosorption pattern was observed for the uptake of Cr(VI) ions by the presence of increasing concentrations of Cd(II) ions when empirically selected initial concentrations of Cu(II) ions were chosen as parameters. However, the Cd(II) uptake was more severely affected by the presence of Cr(VI). The effect of different levels of Cr(VI) and Cu(II) on the uptake of Cd(II) is quantitatively much better demonstrated in Fig. 6, showing how the uptake of Cd(II) decreased in the presence of Cr(VI) and Cu(II). The curves in Fig. 6 represent series of Cr(VI) ‘isoconcentration cuts’ of the Cd(II) biosorption surface in Fig. 5(b). At low Cd(II) levels, Cr(VI) and Cu(II) affected the Cd(II) uptake very strongly, but the effect was less at higher Cd(II) concentrations. There is a marked difference between the shape of the two isotherm surfaces for the Cu(II)+Cr(VI) and Cd(II)+Cr(VI) systems as illustrated in Figs. 2(b) and 5(b), respectively. Since the uptake of Cu(II) ions was less affected with increasing concentrations of Cr(VI) ions, the Cu(II)+Cr(VI) biosorption surface was curved convexly upward. On the other hand, the Cd(II) uptake was more severely affected by the presence of Cr(VI) and, the Cd(II)+Cr(VI) biosorption surface was curved concavely downward.

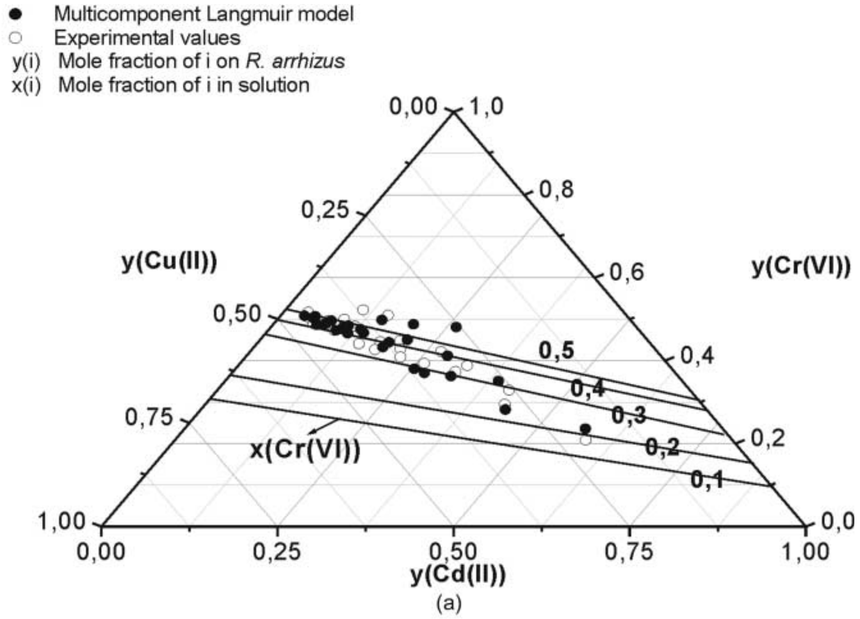

***Figure 1.*** Graphical representation of triangular equilibrium diagrams for the biosorption of Cr(VI), Cu(II), and Cd(II) ions on *R. arrhizus* from ternary metal mixtures using multicomponent Langmuir model. (a) Biosorption isotherms of the constant Cr(VI) fraction in solution (—); (b) Biosorption isotherms of the constant Cu(II) fraction in solution (—); (c) Biosorption isotherms of the constant Cd(II) fraction in solution (—).

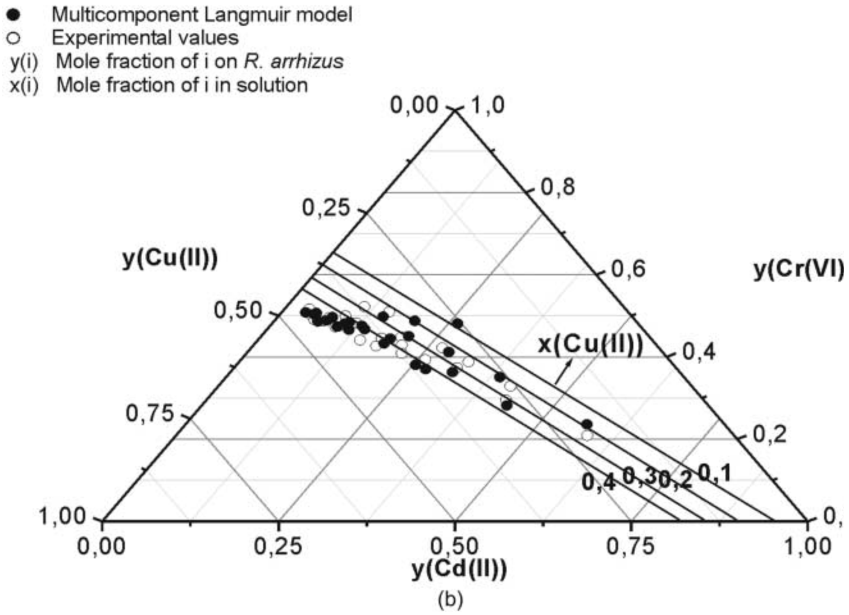

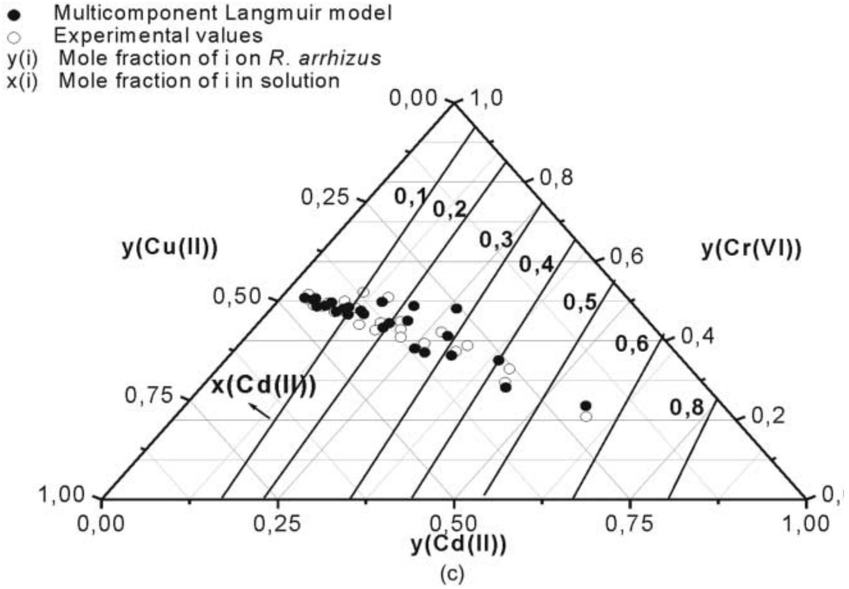

*Figure 1*. Continued.

Finally, the triangular equilibrium diagram was constructed again by using the multicomponent Freundlich model. Large deviations from the multicomponent Freundlich model observed for Cr(VI) ions were much more pronounced in the triangular equilibrium diagram (Fig. 7).

## Quantitative Analysis of Selective Biosorption in Ternary Systems

The selectivity of *R. arrhizus* for Cr(VI), Cu(II), and Cd(II) in the ternary mixtures was evaluated in terms of the relative metal $i$ biosorption $R_i$ (%), the individual and total biosorption efficiencies $Y_i$ and $Y_t$ (%), respectively, and the relative coverage $\theta_i$ (%). As can be seen from Table 6, the total interactive effects of Cr(VI), Cu(II), and Cd(II) ions on the biosorption of Cr(VI) by *R. arrhizus* were generally synergistic ($R > 100$), whereas the presence of these metal ions together strongly inhibited the uptake of Cd(II) ions. Cu(II) and Cd(II) ions

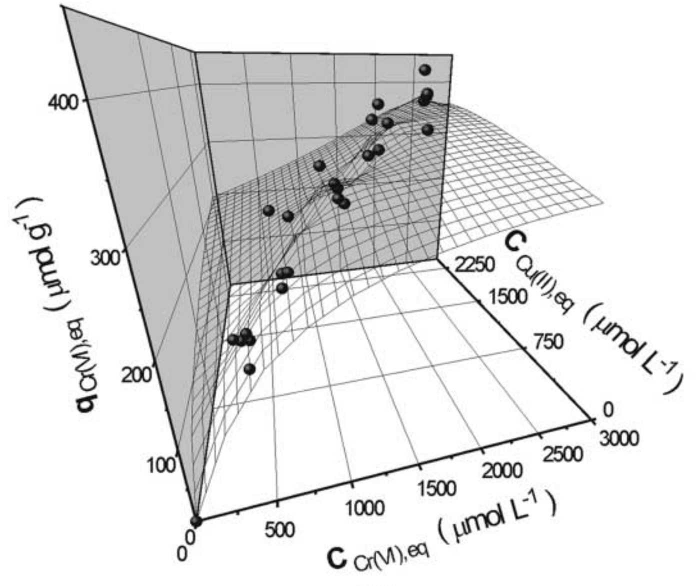

(a)

***Figure 2.*** Three-dimensional biosorption isotherm surfaces created by using multicomponent Langmuir model for the Cr(VI)+Cu(II)+Cd(II) systems with $C_{\mathrm{Cd,eq}}$ as a parameter. (a) The effect of Cu(II) on equilibrium uptake of Cr(VI). (b) The effect of Cr(VI) on equilibrium uptake of Cu(II). (c) The effect of Cr(VI) and Cu(II) on equilibrium total Cr(VI)+Cu(II) uptake.

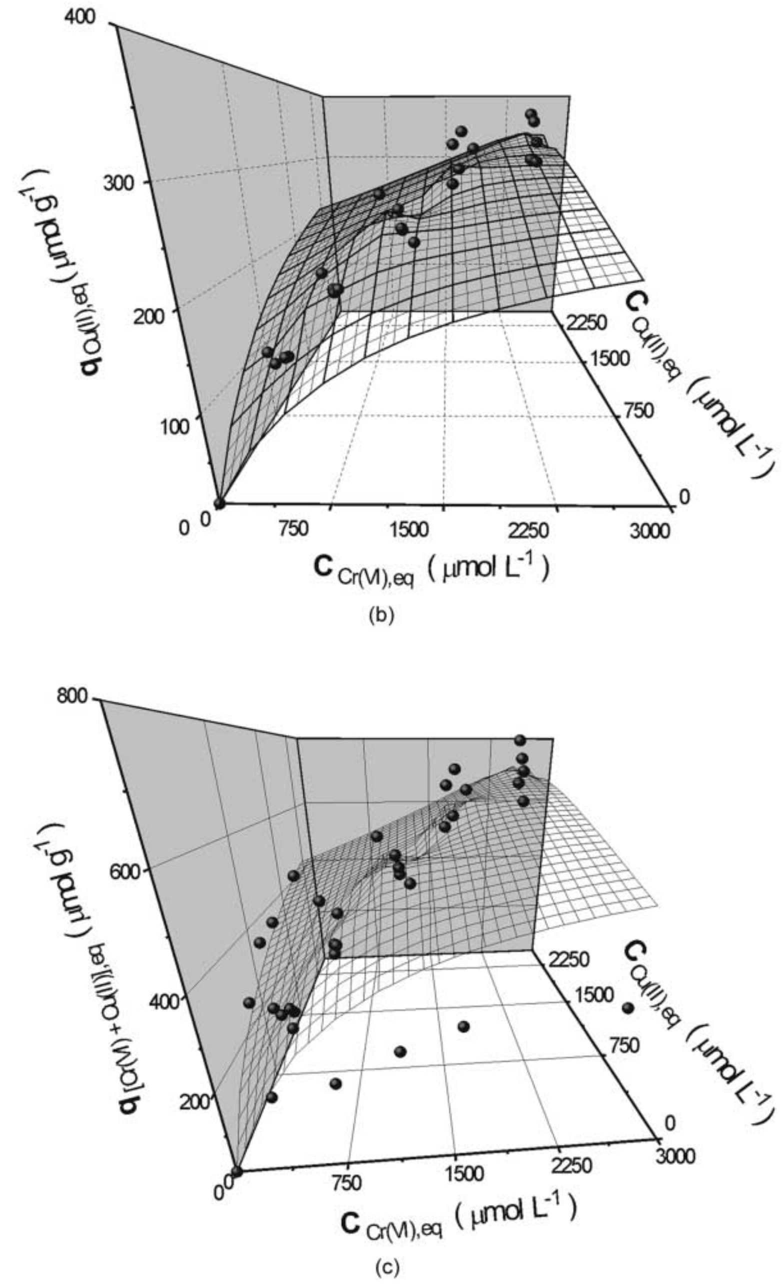

***Figure 2***. Continued.

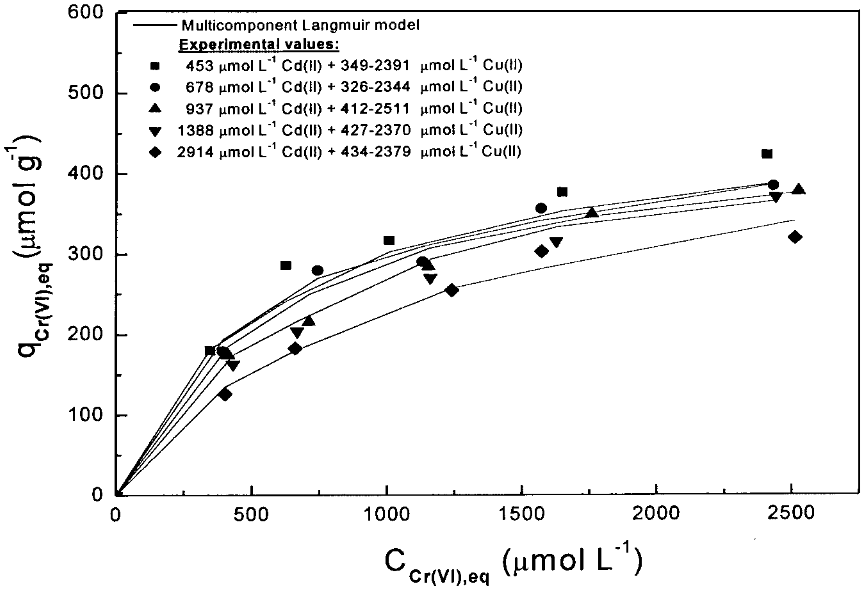

***Figure 3.*** The effect of Cu(II) and Cd(II) on the uptake of Cr(VI). The multicomponent Langmuir model profiles are presented in full lines, the symbols denote experimentally obtained values.

showed generally antagonistic interaction. The degree of competition in the case of Cu(II) was small in most instances so that the amount of bound Cu(II) was $\geq 77\%$ of its amount bound when added singly. A somewhat more antagonistic effect was observed with Cd(II) in the presence of Cr(VI) and Cu(II). It is also interesting to note that the relative Cd(II) biosorption increased and synergistic interaction was observed when the Cd(II) ion concentration and/or the ratio of the Cd(II) ion concentration was increased with respect to the Cr(VI) and Cu(II) ion concentrations and/or the total metal ion concentration. The order of inhibition of Cu(II) and Cd(II) biosorption in different three-metallic combinations as compared to single metallic species suggested in favor of screening or competition for the binding sites on the cellular surface. The synergistic behavior of Cr(VI) and partially Cd(II), observed at higher concentrations of the Cd(II) ions, may be due to the large difference in concentration between the biosorbent surface and multimetal solution or strong driving force, compared with the single-metal system.

According to the results shown in Table 6, an increase in the initial metal concentration led to a decrease in the biosorption efficiency of each metal. This

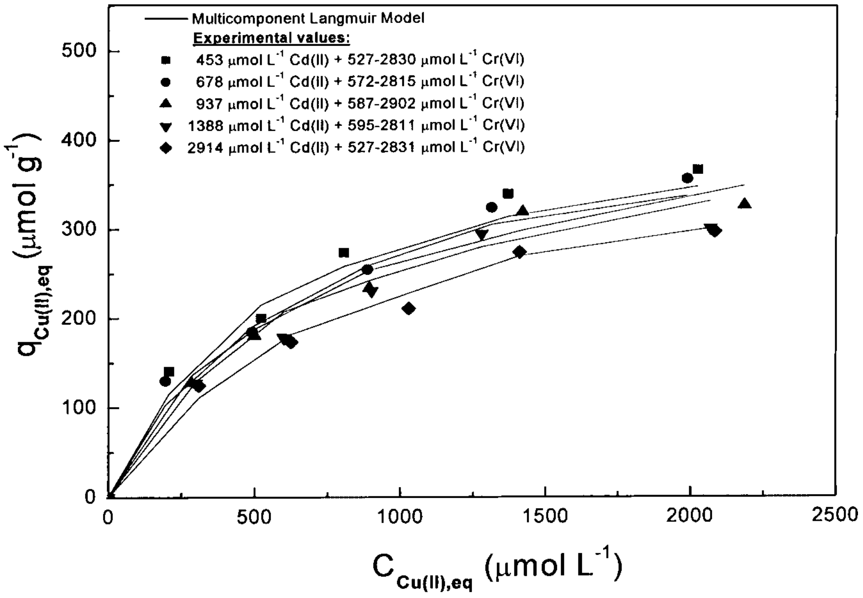

***Figure 4.*** The effect of Cr(VI) and Cd(II) on the uptake of Cu(II). The multicomponent Langmuir model profiles are presented in full lines, the symbols denote experimentally obtained values.

trend seems reasonable since the relative number of binding sites available to each metal would reduce as the concentrations of the three metals were increased simultaneously, particularly when the biomass was nearly saturated at high initial concentrations. The biosorption efficiency of the three metals was in the order $Y_{Cu}\% > Y_{Cr}\% > Y_{Cd}\%$. Since the Cd(II) uptake was strongly inhibited by the presence of Cr(VI) and Cu(II) ions, the individual Cd(II) biosorption efficiency was also lower than the total biosorption efficiency for all metal ion concentration combinations detected.

Cr(VI) ions had the highest relative coverage ($\theta_{Cr}\%$) of 43–51% in the ternary mixtures containing approximately equal molar concentrations of Cr(VI), Cu(II), and Cd(II) ions. The relative coverage of Cu(II) ($\theta_{Cu}\%$) was slightly lower with a value of 34–41%, while the value of $\theta_{Cd}\%$ was the lowest (15–21%) among the three metals. The relative coverage of the Cr(VI) and Cu(II) ions did not vary considerably at all concentrations detected, while the relative coverage of the Cd(II) ions depended on the molar concentration ratio, e.g., when the ratio of the Cd(II) ion concentration to the Cr(VI) and Cu(II) ion concentrations, $C_{Cd,i}/C_{Cr,i}/C_{Cu,i}$, was chosen as 1/(1/5)/(1/6), a maximum relative coverage for

Cd(II) ions was obtained as 58.3%. The dominance of selective biosorption according to the relative coverage data was in the order Cr(VI) > Cu(II) > Cd(II).

Factors that affect the biosorption preference of a biosorbent for metals are related to the physicochemical parameters of the solution (e.g., pH, temperature, etc.), and specific surface properties of the microorganism (e.g., functional groups, structure, etc.). Binding of different metal ions on biomaterials having different functional groups depends on also some physical and chemical properties of metals (Table 7). Since the movement of metals with a higher atomic weight can generate higher momentum energy, which may promote the biosorption of the metal by increasing the probability of effective collision between the metal and the biosorbent surface, a higher atomic weight leads to a higher biosorption preference by the biosorbent. The data presented do not support this proposal. Another general rule in heavy metal biosorption is that the higher charged the ions, the higher the affinity. The Cu(II) ions have $d^9$ electronic configuration, and unpaired electrons. They are capable of being attracted to a

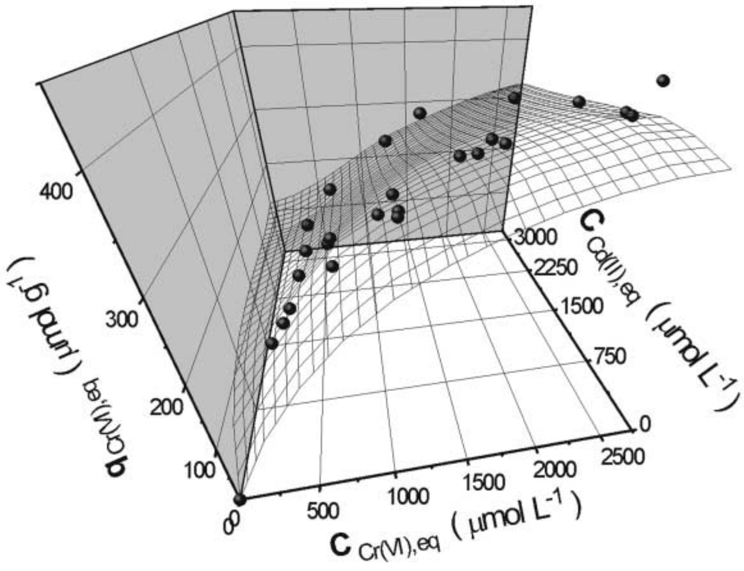

(a)

***Figure 5.*** Three-dimensional biosorption isotherm surfaces created by using multicomponent Langmuir model for the Cr(VI)+Cu(II)+Cd(II) systems with $C_{\mathrm{Cu,eq}}$ as a parameter. (a) The effect of Cd(II) on equilibrium uptake of Cr(VI). (b) The effect of Cr(VI) on equilibrium uptake of Cd(II). (c) The effect of Cr(VI) and Cd(II) on equilibrium total Cr(VI)+Cd(II) uptake.

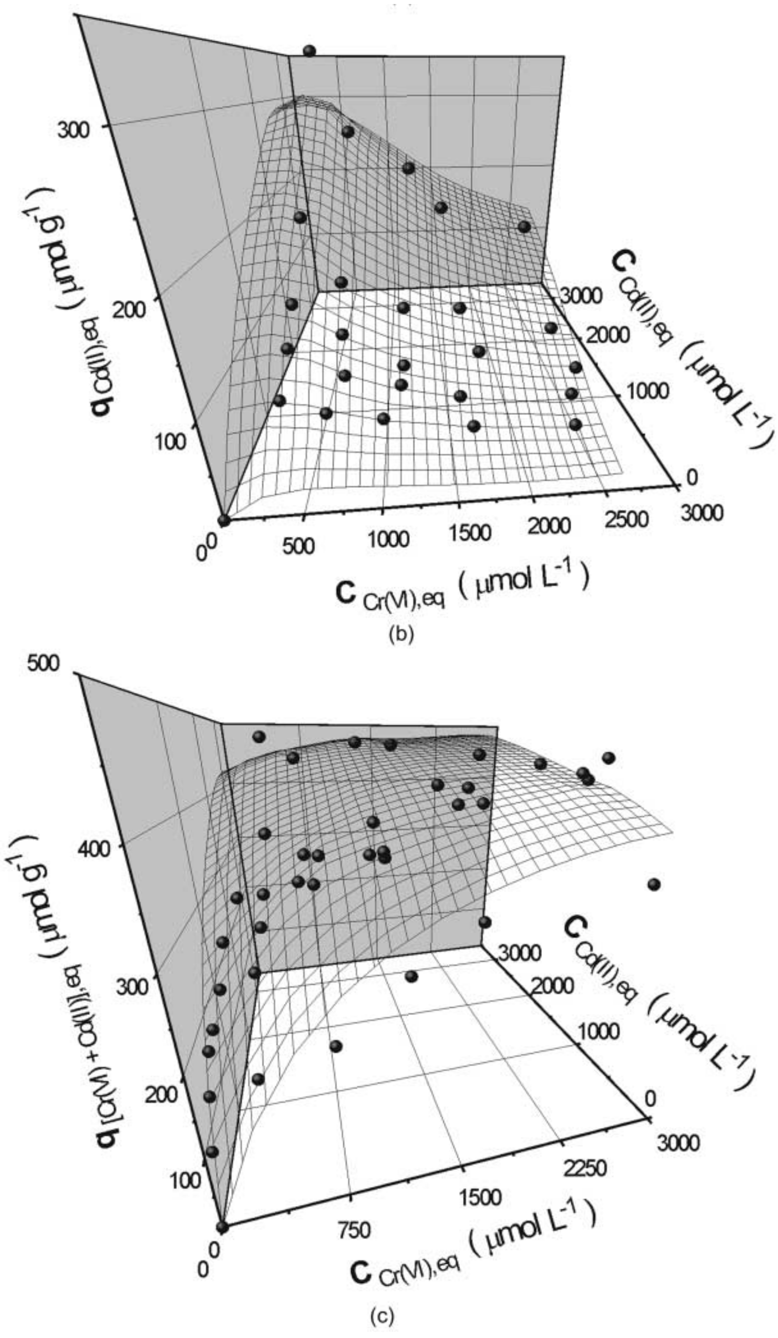

(b)

(c)

***Figure 5***. Continued.

Marcel Dekker, Inc.
270 Madison Avenue, New York, New York 10016

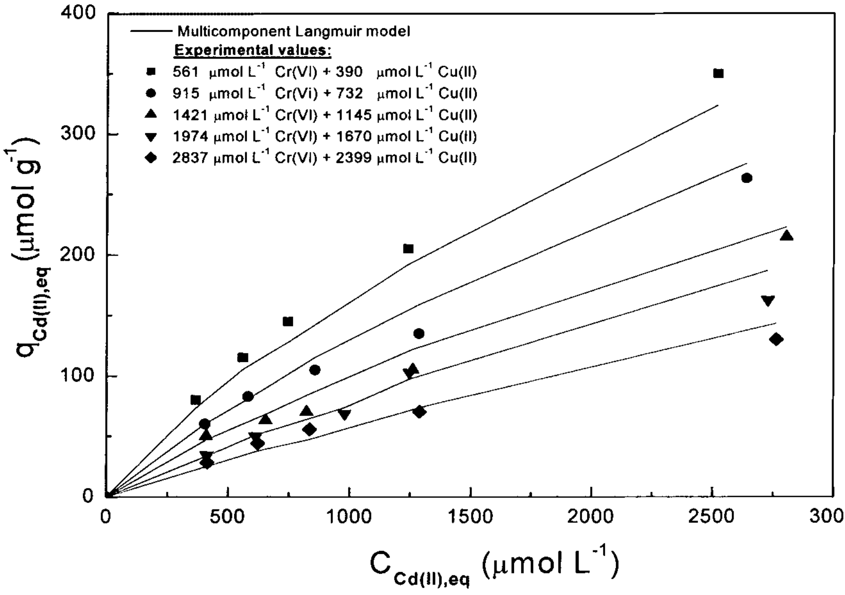

*Figure 6.* The effect of Cr(VI) and Cu(II) on the uptake of Cd(II). The multicomponent Langmuir model profiles are presented in full lines, the symbols denote experimentally obtained values.

magnetic field possibly originating from the biosorbent. The Cu(II) ions form distorted octohedral complexes. Binding of Cu(II) ions involve the exchange of one or two aquoligands by carboxylate oxygens (29,30). This complex is reported to involve chelation with the carboxylic group on the basis of IR analysis (30,31). The sorption mechanism for Cu(II) is different from Cd(II) and other divalent metals. Cd(II) ions have $d^{10}$ electronic configuration, and are very stable (no unpaired electron), and slightly repelled by a magnetic field. The chemical bonds tend to be isotopic and polyhedra are generally regular (30,32). Moreover, there are two possible coordination numbers [2,4] associated with Cu(II) as compared to only one for Cd(II) [4]. If the systems form complexes in the biosorbent phase, then Cu(II) (the least stable among the three metals examined) only required two more electrons to do so as compared with Cd(II) which requires four electrons. Cd(II) forms octahedral complexes and these are more stable because Cd(II) is larger. More electronegative metal ions will be more strongly attracted to the surface. The sorption capacity of Cd(II) is smaller than Cu(II) also due to its low electronegativity. On the other hand, Cd(II) ions are more electronegative than Cr(VI) ions, but they are sorbed the least. Another factor is the ionic radius itself, especially since a smaller ionic radius implies more molecules can sorb onto a fixed surface area of biosorbent. The fact that Cr(VI) has the smallest ionic radius, and it is the most sorbed ion in a wide pH range among the three ions examined. The other metal ions also follow this trend. Metals with a higher reduction potential tend to exhibit a stronger ionic interaction with an electron-rich surface of biosorbents. This trend is also reflected. Our findings on the order of biosorption preference of Cr(VI), Cu(II), and Cd(II) is essentially consistent with the correlation between the chemical and physical properties of the metal ions and the selective biosorption with only one exception, atomic weight. It is generally complicated to find a common rule to identify how metal properties affect the competitive biosorption. This is because the observed behavior may result from a combination of all the above factors. Moreover, the characteristics of biosorbents and the variations in composition and structure of the biosorbent surface by changing physicochemical parameters of the solution also affect the order of metal biosorption preference.

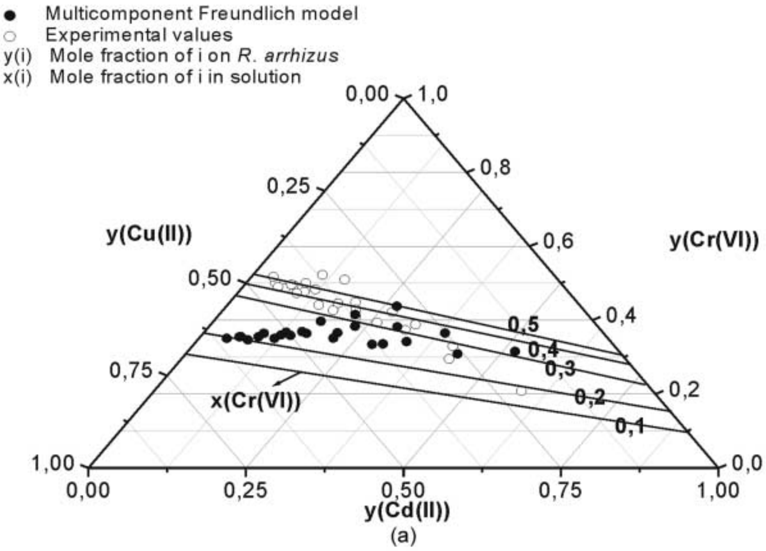

*Figure 7.* Graphical representation of triangular equilibrium diagrams for the biosorption of Cr(VI), Cu(II), and Cd(II) ions on *R. arrhizus* from ternary metal mixtures using multicomponent Freundlich model. (a) Biosorption isotherms of the constant Cr(VI) fraction in solution (—); (b) Biosorption isotherms of the constant Cu(II) fraction in solution (—); (c) Biosorption isotherms of the constant Cd(II) fraction in solution (—).

(*continued*)

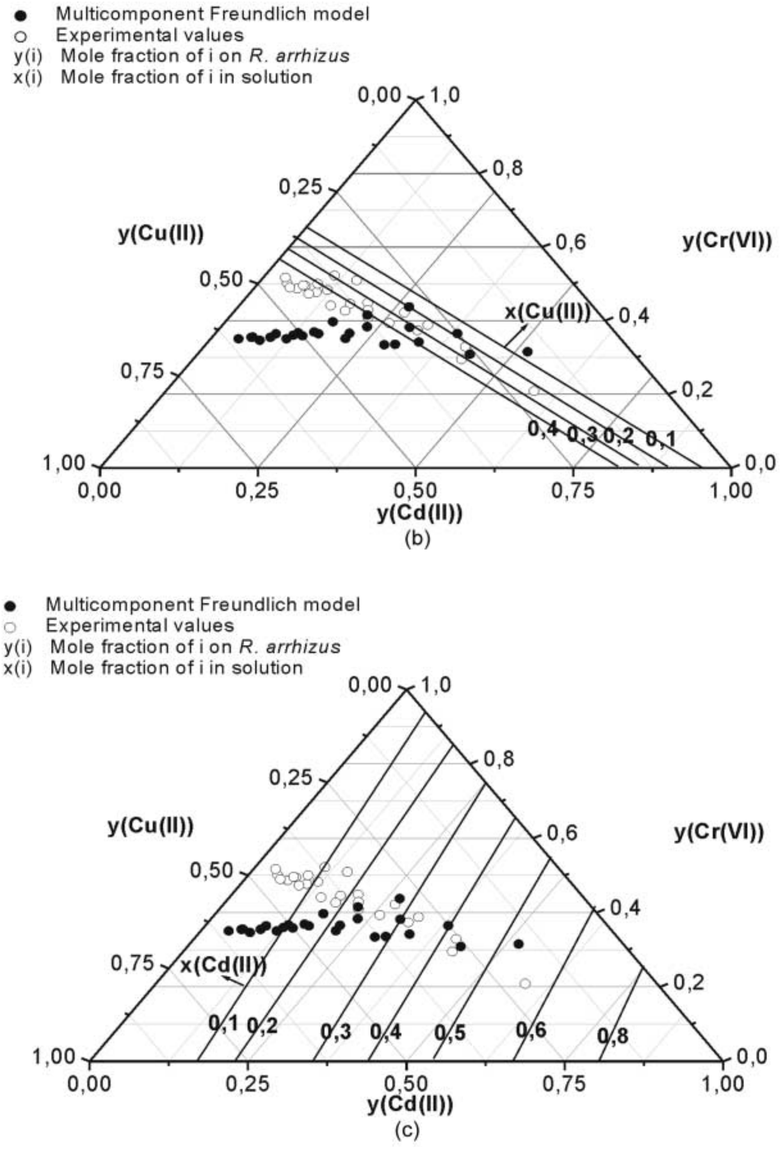

*Figure 7*. Continued.

**Table 6.** Comparison of Cr(VI), Cu(II), and Cd(II) Biosorption Capacity of *R. arrhizus* in Terms of the Relative Metal Biosorption, the Individual and Total Biosorption Efficiencies, and the Relative Coverage

| $C_{Cd,o}$ ($\mu$mol $L^{-1}$) | $C_{Cr,o}$ ($\mu$mol $L^{-1}$) | $C_{Cu,o}$ ($\mu$mol $L^{-1}$) | $R_{Cd}$ (%) | $Y_{Cd}$ (%) | $\theta_{Cd}$ (%) | $R_{Cr}$ (%) | $Y_{Cr}$ (%) | $\theta_{Cr}$ (%) | $R_{Cu}$ (%) | $Y_{Cu}$ (%) | $\theta_{Cu}$ (%) | $Y_t$ (%) |
|---|---|---|---|---|---|---|---|---|---|---|---|---|
| 448 | 527 | 349 | 64.1 | 17.9 | 20.0 | 98.9 | 34.2 | 44.9 | 82.5 | 40.4 | 35.2 | 30.3 |
| 891 | 587 | 412 | 87.7 | 16.3 | 32.5 | 95.5 | 29.6 | 38.9 | 74.9 | 31.1 | 28.7 | 23.7 |
| 2869 | 527 | 434 | 159.1 | 12.2 | 58.3 | 68.9 | 23.8 | 20.9 | 73.0 | 28.8 | 20.8 | 15.7 |
| 467 | 911 | 723 | 48.1 | 12.9 | 11.0 | 140.0 | 31.4 | 52.3 | 78.7 | 27.7 | 36.7 | 26.0 |
| 963 | 926 | 681 | 63.6 | 10.9 | 21.0 | 105.3 | 23.2 | 42.9 | 70.9 | 26.5 | 36.1 | 19.5 |
| 2902 | 843 | 799 | 119.5 | 9.1 | 42.5 | 89.4 | 21.6 | 29.5 | 68.0 | 21.7 | 28.0 | 13.6 |
| 461 | 1325 | 1080 | 40.0 | 10.8 | 7.8 | 118.5 | 23.9 | 49.5 | 79.3 | 25.3 | 42.7 | 22.3 |
| 1366 | 1430 | 1133 | 59.1 | 7.7 | 17.3 | 101.1 | 18.9 | 44.6 | 66.9 | 20.4 | 38.1 | 15.4 |
| 3018 | 1493 | 1241 | 97.5 | 7.1 | 31.6 | 95.2 | 17.0 | 37.4 | 61.1 | 17.0 | 31.0 | 11.8 |
| 447 | 2024 | 1710 | 27.7 | 7.7 | 4.6 | 120.0 | 18.5 | 50.1 | 95.4 | 19.8 | 45.2 | 17.9 |
| 1049 | 2107 | 1740 | 41.7 | 6.6 | 9.4 | 111.2 | 16.5 | 47.3 | 89.6 | 18.3 | 43.3 | 15.0 |
| 2890 | 1874 | 1684 | 74.0 | 5.6 | 22.0 | 96.4 | 16.1 | 40.9 | 77.1 | 16.2 | 37.1 | 11.5 |
| 444 | 2830 | 2390 | 22.8 | 6.4 | 3.5 | 126.2 | 14.9 | 51.7 | 88.8 | 15.3 | 44.8 | 14.4 |
| 891 | 2902 | 2511 | 33.6 | 6.2 | 7.4 | 112.6 | 13.0 | 49.7 | 79.1 | 12.9 | 43.0 | 12.0 |
| 2893 | 2830 | 2379 | 59.1 | 4.5 | 17.5 | 95.2 | 11.2 | 42.7 | 72.1 | 12.4 | 39.8 | 9.2 |

***Table 7.*** Correlation of Some Physical and Chemical Properties of Metals with Metal Biosorption Selectivity

| | Cr | Cu | Cd |
|---|---|---|---|
| Atomic weight | 52.00 | 63.55 | 112.41 |
| Charge | $6^+$ | $2^+$ | $2^+$ |
| Electron configuration | $3d^5 4s^1$ | $3d^{10} 4s^1$ | $4d^{10} 5s^2$ |
| $M^{2+}$ | $3d^4$ | $3d^9$ | $4d^{10}$ |
| $M^{3+}$ | $3d^3$ | – | – |
| $M^{6+}$ | $3p^6$ | – | – |
| Electronegativity of the atom | 1.66 | 1.90 | 1.69 |
| Ionic radius (Å) | 0.52 | 0.72 | 0.95 |
| Standard reduction potential (V) | $Cr^{6+} + 3e^- \rightarrow Cr^{3+}$ 1.10<br>$Cr^{3+} + 3e^- \rightarrow Cr$ −0.74 | $Cu^{2+} + 2e^- \rightarrow Cu$ 0.340 | $Cd^{2+} + 2e^- \rightarrow Cd$ −0.403 |

## CONCLUSIONS

Equilibrium metal uptake performance of *R. arrhizus* was studied using aqueous solutions containing Cr(VI), Cu(II), and Cd(II) ions in single-metal systems and ternary metal mixtures. Although the procedure of fitting the multicomponent Langmuir model to the ternary data is semiempirical and the information provided from maximal capacities seems to violate basic assumptions of the multicomponent Langmuir model, predictions of the behavior of Cr(VI)–Cu(II)–Cd(II) ternary metal system were in a reasonably good agreement with experimental results. The multicomponent Freundlich model showed good fits for the competitive Cu(II)–Cd(II) biosorption data, whereas the model had larger deviations on interpreting ternary biosorption data of Cr(VI) ions. The magnitude of the multicomponent Langmuir constant, $K_i$, followed a trend of Cu(II) > Cr(VI) > Cd(II). The same order of selectivity was obtained in terms of the individual biosorption efficiency, in agreement with the single-component data at pH 4.0, whereas in three metal biosorption, the relative metal *i* biosorption and the relative coverage of the metals decreased in order of Cr(VI) > Cu(II) > Cd(II).

## REFERENCES

1. Volesky, B. Biosorption by Fungal Biomass. In *Biosorption of Heavy Metals*; Volesky, B., Ed.; CRC Press: Boca Raton, FL, 1990; 139–172.
2. Volesky, B. Advances in Biosorption of Metals: Selection of Biomass Types. FEMS Microbiol. Rev. **1994**, *14*, 291–302.
3. Williams, C.J.; Aderhold, D.; Edyvean, R.G.J. Comparison Between Biosorbents for the Removal of Metal Ions from Aqueous Solutions. Wat. Res. **1998**, *32* (1), 216–224.
4. Aksu, Z. Biosorption of Heavy Metals by Microalgae in Batch and Continuous Systems. In *Waste Water Treatment with Algae*; Wong, Y.-S., Tam, N.F.Y., Eds.; Springer-Verlag: Berlin, 1998; 37–55.
5. Yerushalmi, L. Propagation of Biosorbents by Fermentation Processes. In *Biosorption of Heavy Metals*; Volesky, B., Ed.; CRC Press: Boca Raton, FL, 1990; 341–358.
6. Patterson, J.W. *Waste Water Treatment*; Science Publishers: New York, 1977; 38–39, see also pp. 53–75, 91–114.
7. Ting, Y.P.; Lawson, F.; Prince, I.G. Uptake of Cadmium and Zinc by the Alga *Chlorella vulgaris*: II. Multi-ion Situation. Biotechnol. Bioengng **1991**, *37*, 445–455.
8. Chong, K.H.; Volesky, B. Metal Biosorption Equilibria in a Ternary System. Biotechnol. Bioengng **1996**, *49*, 629–638.

9. Schiewer, S.; Volesky, B. Modeling Multi-metal Ion Exchange in Biosorption. Environ. Sci. Technol. **1996**, *30*, 2921–2927.
10. Sağ, Y.; Kutsal, T. Fully Competitive Biosorption of Chromium(VI) and Iron(III) Ions from Binary Metal Mixtures by *R. arrhizus*: Use of the Competitive Langmuir Model. Process Biochem. **1996**, *31* (6), 573–585.
11. Sağ, Y.; Kutsal, T. The Selective Biosorption of Chromium(VI) and Copper Ions from Binary Metal Mixtures by *R. arrhizus*. Process Biochem. **1996**, *31* (6), 561–572.
12. Figueira, M.M.; Volesky, B.; Ciminelli, V.S.T. Assessment of Interference in Biosorption of a Heavy Metal. Biotechnol. Bioengng **1997**, *54*, 344–350.
13. Sağ, Y.; Kutsal, T. The Simultaneous Biosorption of Cr(VI), Fe(III) and Cu(II) on *Rhizopus arrhizus*. Process Biochem. **1998**, *33* (5), 571–579.
14. Chong, K.H.; Volesky, B. Description of Two-Metal Biosorption Equilibria by Langmuir-Type Models. Biotechnol. Bioengng **1995**, *47*, 451–460.
15. de Carvalho, R.P.; Chong, K.-H.; Volesky, B. Evaluation of the Cd, Cu and Zn Biosorption in Two-Metal Systems Using Algal Biosorbent. Biotechnol. Prog. **1995**, *11*, 39–44.
16. Sağ, Y.; Açıkel, Ü.; Aksu, Z.; Kutsal, T. A Comparative Study for the Simultaneous Biosorption of Cr(VI) and Fe(III) on *C. vulgaris* and *R. arrhizus*: Application of the Competitive Adsorption Models. Process Biochem. **1998**, *33* (3), 273–281.
17. Snell, F.D.; Snell, C.T.; *Colorimetric Methods of Analysis*; 3rd Ed.; Van Nostrand: New York, 1959; Vol. 2, 1–46; see also pp. 78–139.
18. Hayward, D.O.; Trapnell, B.M.W. *Chemisorption*, 2nd Ed.; Butterworths: London, 1964; 67–159.
19. Smith, J.M. *Chemical Engineering Kinetics*; 3rd Ed.; McGraw-Hill: New York, 1981; 310–326.
20. Bellot, J.C.; Condoret, J.S. Modelling of Liquid Chromatography Equilibria. Process Biochem. **1993**, *28*, 365–376.
21. Yang, R.T. *Gas Separation by Adsorption Processes*; Butterworths: Boston, 1987; 49.
22. Sheindorf, C.H.; Rebhun, M.; Sheintuch, M. A Freundlich-Type Multicomponent Isotherm. J. Colloid Interface Sci. **1981**, *79* (1), 136–142.
23. Sheindorf, C.H.; Rebhun, M.; Sheintuch, M. Organic Pollutants Adsorption from Multicomponent Systems Modeled by Freundlich Type Isotherm. Wat. Res. **1982**, *16*, 357–362.
24. Sheintuch, M.; Rebhun, M. Adsorption Isotherms for Multisolute Systems with Known and Unknown Composition. Wat. Res. **1988**, *22* (4), 421–430.
25. Chang, J.-S.; Chen, C.-C. Quantitative Analysis and Equilibrium Models of Selective Adsorption in Multimetal Systems Using a Bacterial Biosorbent. Sep. Sci. Technol. **1998**, *33*, 611–632.

26. Sağ, Y.; Kutsal, T. The Simultaneous Biosorption Process of Lead(II) and Nickel(II) on *Rhizopus arrhizus*. Process Biochem. **1997**, *32* (7), 591–597.
27. Shallcross, M.; Herrmann, C.C.; McCoy, B.J. An Improved Model for the Prediction of Multicomponent Ion Exchange Equilibria. Chem. Engng Sci. **1988**, *43*, 279–288.
28. Volesky, B.; Holan, Z.R. Biosorption of Heavy Metals. Biotechnol. Prog. **1995**, *11*, 235–250.
29. Bloom, P.R.; McBride, M.B. Metal Ion Binding and Exchange with Hydrogen Ions in Acid Washed Peat. Soil Sci. Soc. Am. J. **1979**, *43*, 678–692.
30. Singh, S.; Pradhan, S.; Rai, L.C. Metal Removal from Single and Multimetallic Systems by Different Biosorbent Materials as Evaluated by Differential Pulse Anodic Stripping Voltammetry. Process Biochem. **2000**, *36*, 175–182.
31. Ong, L.H.; Swanson, V.E. Adsorption of Copper by Peat, Lignite and Bituminous Coal. Econ. Geol. **1996**, *61*, 1214–1231.
32. Sarret, G.; Manceau, A.; Spadini, L.; Roux, J.C.; Hazemann, J.L.; Soldo, Y.; Berard, L.E.; Menthonnex, J.J. Structural Determination of Zn and Pb Binding Sites in *Penicillium chrysogenum* Cell Walls by EXAFS Spectroscopy. Environ. Sci. Technol. **1998**, *32*, 1648–1655.

Received December 2000
Revised May 2001

## Request Permission or Order Reprints Instantly!

Interested in copying and sharing this article? In most cases, U.S. Copyright Law requires that you get permission from the article's rightsholder before using copyrighted content.

All information and materials found in this article, including but not limited to text, trademarks, patents, logos, graphics and images (the "Materials"), are the copyrighted works and other forms of intellectual property of Marcel Dekker, Inc., or its licensors. All rights not expressly granted are reserved.

Get permission to lawfully reproduce and distribute the Materials or order reprints quickly and painlessly. Simply click on the "Request Permission/Reprints Here" link below and follow the instructions. Visit the U.S. Copyright Office for information on Fair Use limitations of U.S. copyright law. Please refer to The Association of American Publishers' (AAP) website for guidelines on Fair Use in the Classroom.

The Materials are for your personal use only and cannot be reformatted, reposted, resold or distributed by electronic means or otherwise without permission from Marcel Dekker, Inc. Marcel Dekker, Inc. grants you the limited right to display the Materials only on your personal computer or personal wireless device, and to copy and download single copies of such Materials provided that any copyright, trademark or other notice appearing on such Materials is also retained by, displayed, copied or downloaded as part of the Materials and is not removed or obscured, and provided you do not edit, modify, alter or enhance the Materials. Please refer to our Website User Agreement for more details.

**Order now!**

Reprints of this article can also be ordered at

http://www.dekker.com/servlet/product/DOI/101081SS120000789

Downloaded At: 10:37 25 January 2011